Asian Journal of Chemistry; Vol. 37, No. 2 (2025), 369-376

ASIAN JOURNAL OF CHEMISTRY

https://doi.org/10.14233/ajchem.2025.33047

DFT Studies, Structural Investigation and *in vitro* Biological Evaluation of Binary Metal Complexes Derived from (*R*)-*N*-Phenyl Ethylamine and 2-Hydroxy-1-naphthaldehyde

JAGADISH TOTA[1,*], ESHWARI KASOJI[2], ANITHA RANGA SREE DOMA[3], KADEER MOHAMAD[1] and MALLESH DOSALI[1]

[1]Department of Chemistry (H&S), CVR College of Engineering, Hyderabad-501510, India
[2]G. Narayanamma Institute of Technology and Science, Shaikpet, Hyderabad-500104, India
[3]Department of Chemistry, Nizam College, Osmania University, Hyderabad-500001, India

*Corresponding author: E-mail: jagadish.tota123@gmail.com

Received: 15 November 2024; *Accepted*: 8 January 2025; *Published online*: 31 January 2025; AJC-21888

The chiral Schiff base (HL) derived from 2-hydroxy-1-naphthaldehyde and N-phenyl ethylamine and its metal complexes. Co(II), Ni(II) and Cu(II) were synthesized and characterized by the molar conductance, TGA, FT-IR, UV-visible and mass spectral techniques. Gauss-View screen was used to visualize all the synthesized compounds using Gaussian 09 software. Molecular electrostatic potentials, frontier molecular orbitals, the 6-311++G (d,p) basis set for the ligand, as well as SDD basis sets for its metal complexes, were used in the DFT/B3LYP functional analysis in order to investigate the most probable stability of the HL ligand and its complex based on E_{HOMO} and E_{LUMO} values. As a first step in screening for *in vitro* antibacterial activity against Gram-positive and Gram-negative bacteria, the disc diffusion assay was employed, while the cytotoxicity of the synthesized compounds was assessed using the MTT assay. Cobalt(II) complex showed strong antibacterial properties against *P. putida* and *B. subtilis* strains, while Cu(II) complex showed significant antitumor activity against MCF-7 and HeLa strains.

Keywords: Binary complexes, HOMO-LUMO, MEP, Antibacterial activity, Anticancer activity.

INTRODUCTION

In coordination chemistry, the metal complexes of Schiff base ligands are regarded as models for the active sites of enzymes [1] and have a wide range of applications such as anti-inflammatory [2,3], anticancer [4,5], antimicrobial [6,7], anti-diabetic [8], *etc*. The metal complexes are also acts as good catalytic applications in the reactions like polymerization, olefin oxidation and also most of the zinc complexes act as good catalysts in three or four component reaction in multi-component reactions (MCRs) [9-11]. Recently, significant attention has been placed on Schiff base metal complexes as catalysts for oxygen reduction, which is crucial in fuel cell technology and pharmaceutical formulation [12,13]. The biological activity of metal complexes is mainly due to the azomethine linkage present in their ligands.

The Schiff bases complexes are also used as effective scavengers of reactive oxygen species, which is an antioxidant compound [14]. Density functional theory (DFT) has been more popular in recent decades due to the fact that it describes the structure and spectra of an electron density-dependent system [15]. Quantum chemical descriptors, molecule electrostatic potential and energy of boundary molecular orbitals are the significant tools for evaluating antibiotic inhibitory performances [16]. In present article, a chiral Schiff base ligand and its correspoding metal complexes was synthesized and characterized using using spectroscopic and analytical techniques. The combination of computational and experimental studies will lead to a more precise and organized comprehension of the compounds being studied. Therefore, the purpose of this study is to use spectroscopic and DFT approaches to examine the antibacterial and anticancer capabilities of novel synthesized molecules.

EXPERIMENTAL

All the procured chemicals and solvents were used without additional purification, as supplied by commercial sources. Using a Perkin-Elmer 100S FTIR spectrometer, the vibrational infrared (IR) spectra were measured in the 4000-400 cm^{-1} region

and the UV-visible spectra were measured using a Perkin-Elmer UV-visible spectrophotometer. Hewlett Packard mass spectrometer, Model MS 5988 at 300 ºC and 70 eV was used to measure the mass spectra. At 10^{-3} M, the molar conductivity of the synthesized metal complexes in DMF was measured. The CHNS analysis was recorded using a Vario EL-III CHNS analyzer. In the thermogravimetric analysis of the metal complexes, the heating rate was controlled by 15 ºC min^{-1} using the Mettler Toledo Star system. The Gouy balance was used to determine the magnetic moment values of the metal complexes, with $Hg[Co(NCS)_4]$ acting as the standard.

Synthesis of Schiff base ligand: A mixture of (*R*)-(+)-1-phenylethylamine (1 mmol, 0.121 g) and 2-hydroxy-1-naphthaldehyde (1 mmol, 0.172 g) was suspended in dichloromethane and refluxed for 1.5 h to obtain Schiff base ligand 1-(((1-phenylethyl)imino)methyl)naphthalen-2-ol as a yellow precipitate. After a thorough wash with distilled water, the product was vacuum dried (**Scheme-I**): Yield: 90%. m.p.: 234 ºC. Anal. calcd. (found) % for $C_{19}H_{17}NO$: C, 82.88 (82.90); H, 6.22 (6.18); N, 5.09 (23.45); O, 5.81 (8.77). FT-IR (KBr, ν_{max}, cm^{-1}): 3450 (N-H), 1690 (C=O), 1627 (C=N). ESI-MS *m/z* = 276 $[M]^+$.

Synthesis of metal complexes: A 10 mL methanol was used to dissolve the Schiff base ligand (2 mmol) and the correspoding metal salts (Cu, Co and Ni) (1 mmol). The ligand solution was stirred constantly for 3 to 4 h while adding the coressponding metal salts and then refluxed for 2 h. During cooling, the solid coloured metal complexes precipitated out (**Scheme-II**). Following filtration, washing with methanol and hexane, and vacuum drying, the product was collected using vacuum.

RESULTS AND DISCUSSION

The Schiff base and its metal complexes do not undergo hygroscopically change and are stable at room temperature. Based on the analytical data (Table-1), it is evident that the theoretical values determined for each complex composition are in good agreement with the experimental results. All of the complexes are soluble in dimethyl sulfoxide and dimethyl formamide, despite being insoluble in typical organic solvents.

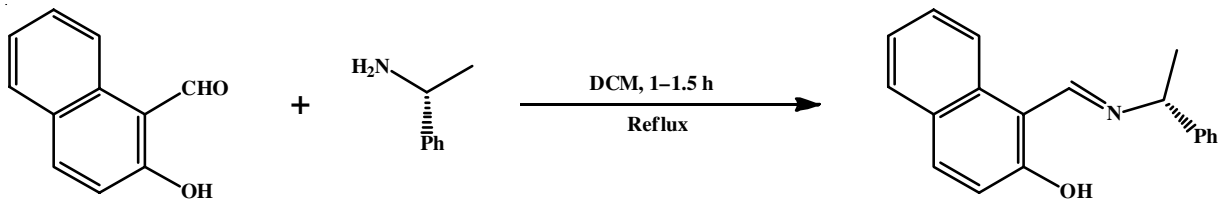

Scheme-I

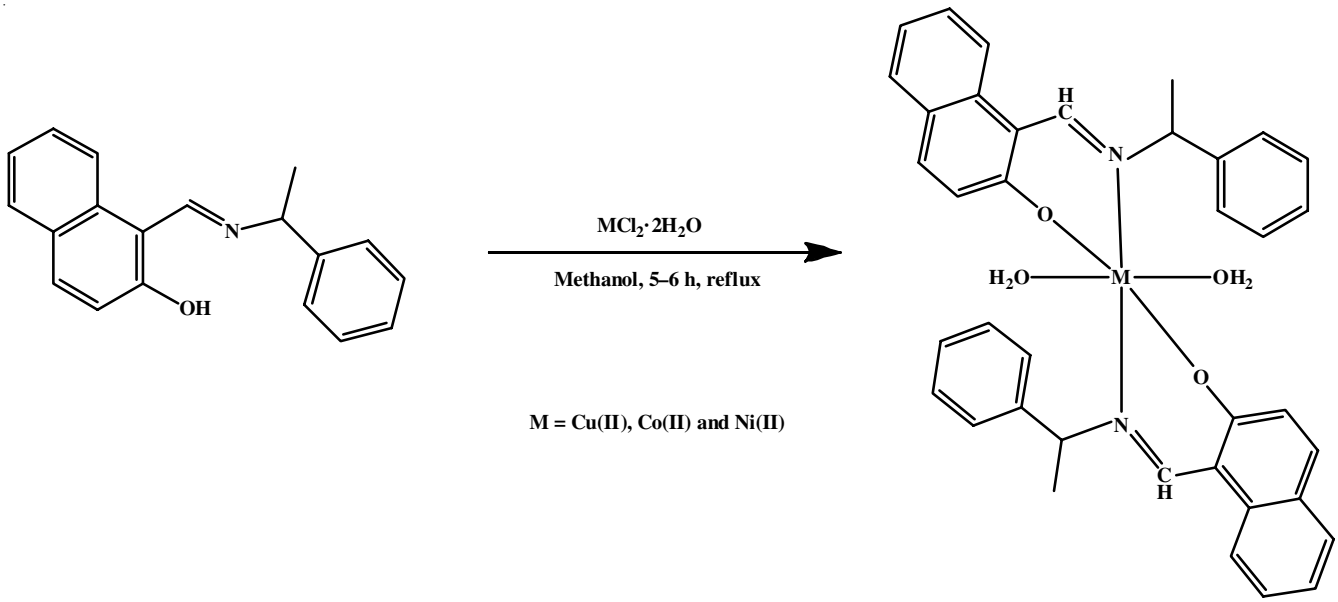

Scheme-II

TABLE-1
ELEMENTAL ANALYSIS OF LIGAND AND ITS METAL COMPLEXES

Formula	m.w.	Elemental analysis (%): Calcd. (found)			
		C	H	N	M
Ligand ($C_{19}H_{17}NO$)	275.0	82.75 (82.90)	6.05 (6.18)	5.08 (5.09)	–
$[Cu(C_{19}H_{16}NO)_2(H_2O)_2]$	647.5	70.12 (70.42)	5.45 (5.56)	8.54 (8.64)	9.65 (9.80)
$[Co(C_{19}H_{16}NO)_2(H_2O)_2]$	643.0	69.56 (70.91)	5.01 (5.59)	3.92 (4.35)	7.96 (9.17)
$[Ni(C_{19}H_{16}NO)_2(H_2O)_2]$	643.0	69.92 (70.91)	4.98 (5.59)	3.96 (4.35)	8.01 (9.17)

Spectral studies: The key IR stretching frequencies of the compounds are shown in Table-2. The ligand showed peak around at 1627 cm^{-1}, which relevant to the azomethine group. In the corresponding Co(II) Ni(II) and Cu(II) complexes, this absorption band has been shifted lowered, which refers that nitrogen is participated in coordination [17]. A broad band at 3448 cm^{-1} correspond to the –OH functional groups of phenol in Schiff base was disappeared in the synthesized complexes, due to coordination of metal ion to phenolic oxygen molecules [18]. But, a low intensity broad band at 3435-3416 cm^{-1} was found in the complexes is due to the intermolecular hydrogen bonding in the complexes [19]. As a result, in metal(II) complexes, the coordinated water molecules showed the diffuse bands at 3192, 3205 and 3192 cm^{-1}, strong absorption bands at 1541, 1541 and 1560 cm^{-1} and weak intensity bands at 827, 825 and 837 cm^{-1} for Ni(II), Cu(II), and Co(II) complexes, respectively [8]. The FTIR spectra of ligand, Cu(II) and Ni(II) complexes are shown in Fig. 1. In ^{1}H NMR spectrum of ligand, the singlet peak observed at δ 15 ppm denoted for the phonolic proton and its high chemical shift could explain by the deshelling effect of Schiff base nitrogen. All the aromatic protons (11 protons) in ligand could appear in between δ 6.9 ppm to δ 7.8 ppm. The singlet peak at about δ 8.8 ppm was observed for the azomethine proton (-CH=N-). The chemical shift at δ 4.6 ppm is due to the asymmetric proton. Moreover, the peak at δ 1.6 ppm is due to the methyl protons. The ligand was produced with its M+1 peak (*m/z* 276) in its mass spectrum and its Cu(II) complex produced its molecular ion peak (*m/z* 647).

Magnetic moment and electronic absorption spectra: Electronic spectra data can be used to identify the geometry of metal complexes and compare them with magnetic moment values. The UV-Vis spectra of the Schiff base ligand and its complexes were measured in DMSO solvent. Two absorption bands are observed for the ligand at 308 and 410 nm. These bands have extended wavelengths due to the coordination of the metal ions. A broad band in the 410-700 nm range has been observed in the Cu(II) complex, suggesting either deformed octahedral geometry or tetragonal geometry [20]. Moreover, the magnetic moment of Cu(II) complex has been measured at 1.86 BM, suggesting distorted octahedral geometry as well. It has been demonstrated that the Co(II) complex exhibits octahedral geometry and defining bands at 435, 551 and 704 nm, corresponding to $^4T_{1g}(F) \rightarrow {}^4T_{1g}(P)$, $^4T_{1g}(F) \rightarrow {}^4A_{2g}(F)$ and $^4T_{1g}(F) \rightarrow {}^4T_{2g}(F)$. The rectangular shape is further supported by the Co(II) complex's magnetic moment value, which was found to be 4.95 BM [21]. For Ni(II) complex, the UV-Vis spectrum showed three bands around at 442, 556 and 712 nm. These could be corresponding to the transitions of $^3A_{2g}(F) \rightarrow {}^3T_{1g}(P)$, $^3A_{2g}(F) \rightarrow {}^3T_{1g}(F)$ and $^3A_{2g}(F) \rightarrow {}^3T_{2g}(F)$. These transitions suggest an octahedral geometry for this complex [22]. All the results are presented Table-3.

TABLE-3
MAGNETIC MOMENT AND ELECTRONIC SPECTRA FOR LIGAND AND THEIR METAL COMPLEXES

Complex	Wavelength (nm)	μ_{eff} (B.M.)
Ligand ($C_{19}H_{17}NO$)	308, 410	–
$[Cu(C_{19}H_{16}NO)_2(H_2O)_2]$	410, 574, 700	1.86
$[Co(C_{19}H_{16}NO)_2(H_2O)_2]$	435, 551, 704	4.95
$[Ni(C_{19}H_{16}NO)_2(H_2O)_2]$	712, 556, 442	3.23

Theoretical studies

Quantum mechanical determinations: A Gaussian O9W software program was used to computationally investigate the quantum-chemical data using DFT (density functional theory). For the ligand, the basis set 6-311++G(d,p) is employed, while for its metal complex counterparts, the basis set SDD was employed. This fundamental functional incorporates the

TABLE-2
IMPORTANT STRETCHING FREQUENCIES OF LIGAND AND ITS METAL COMPLEXES

Schiff base/Complex	ν(OH) (phenolic)	ν(OH) (H_2O)	ν(CH=N) (azomethine)	ν(C–O) (phenolic)	ν(M–O)	ν(M–N)
Ligand ($C_{19}H_{17}NO$)	3448	–	1627	1292	–	–
$[Cu(C_{19}H_{16}NO)_2(H_2O)_2]$	–	3192, 1541, 827	1616	1282	582	462
$[Co(C_{19}H_{16}NO)_2(H_2O)_2]$	–	3205, 1541, 825	1618	1276	586	472
$[Ni(C_{19}H_{16}NO)_2(H_2O)_2]$	–	3192, 1560, 837	1620	1263	586	464

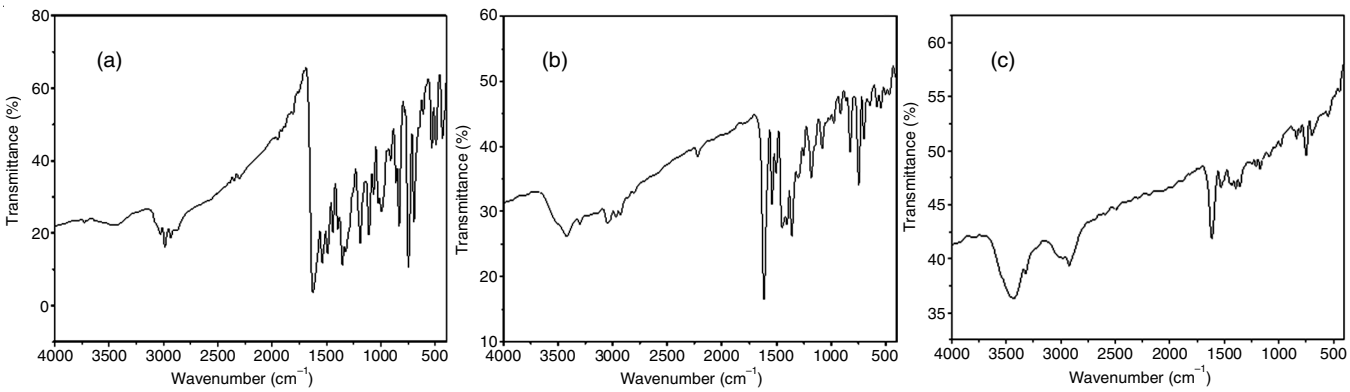

Fig. 1. IR spectra of (a) ligand, (b) Cu(II) and (c) Ni(II) complex

relativistic effects into the computations and is more precise, less expensive and lowers computational costs [23-26]. The optimal molecular geometry, molecular electrostatic potential, frontier molecular orbital and energy band gap are some of the common parameters that were considered. For ligand, Co(II), Cu(II) and Ni(II) metal complexes, the optimized geometric structure was obtained by iteratively solving self-consistent field equations; the global minimum for geometry optimization was found at -864.47499 Hatree, -2025.86987 Hatree, -2077.33333 Hatree and -2050.97186 Hatree, respectively. Table-4 lists the structural characteristics of the metal complex moiety and ligand based on the optimized structures and atom numbering as shown in Figs. 2 and 3.

Frontier molecular orbitals (FMO): The frontier electron density of the Frontier molecular orbital cannot only be used to explain a variety of reactions that occur in the conjugated

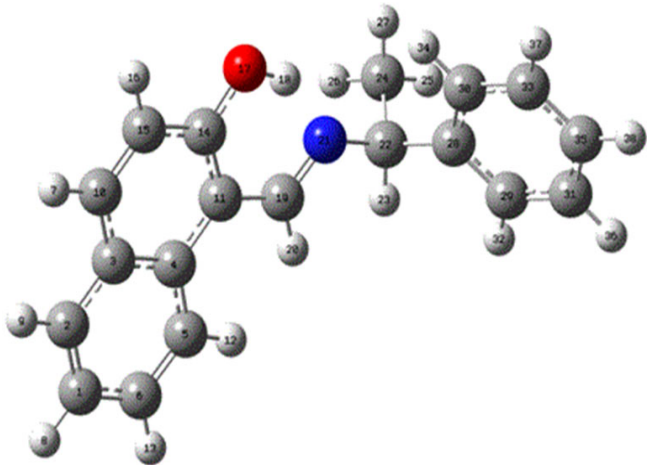

Fig. 2. Optimized structures along with atomic numbering of ligand

TABLE-4
SELECTED BOND LENGTHS OF LIGAND AND ITS METAL COMPLEXES

Ligand		Cu(II)		Co(II)		Ni(II)	
Bond length	Value (Å)	Bond length	Value (Å)	Bond length	Value (Å)	Bond length	Value (Å)
C22-N21	1.46242	Cu1-O39	1.96304	Co81–N55	1.95612	Ni81-N20	1.93440
N21-C19	1.28538	Cu1-N56	1.99775	N55–C56	1.31095	N20-C18	1.30421
C19-H20	1.09390	O39-C40	1.34509	C56-C40	1.44957	C18-C4	1.45419
C19-C11	1.45360	C40-C41	1.42038	C40-C39	1.41977	C4-C2	1.44799
C11-C14	1.40613	C41-C57	1.44941	C39-O38	1.34236	C2-O1	1.36509
C14-O17	1.33663	C57-N56	1.31010	O38-Co81	1.93621	O1-Ni81	1.86593
O17-H18	1.00308	N56- Cu1	1.99775	N55-C61	2.52411	C4-C7	1.39893
Bond angle	Value (°)	C57-H58	1.09382	C39-C41	1.43942	C2-C3	1.39575
C21-C22-C24	109.20650	N56-C59	1.49014	C56-H57	1.09301	C18-H19	1.09031
N21-C22-H23	109.40631	Cu1-O2	1.96361	Co81-O1	1.93548	N20-C21	1.50750
C22-N21-C19	119.19067	Cu1-N21	2.04097	O1-C2	1.34289	Ni81-N55	1.91282
N21-C19-H20	119.28523	O2-C3	1.34761	C2-C4	1.45382	N55-C56	1.31921
N21-C19-C11	122.93426	C3-C5	1.40342	C4-C18	1.45358	C56-H57	1.09002
H20-C19-C11	117.77969	C4-C3	1.40342	C18-N20	1.30987	C56-C40	1.43904
C19-C11-C14	119.17361	C19-N21	1.30694	N20-Co81	1.99524	C40-C39	1.41680
C19-C11-C4	121.67191	N21- Cu1	2.04097	N20-C21	1.51105	C39-O38	1.34332
C4-C11-C14	119.15337	C19-H20	1.09380	C18-H19	1.09273	O38- Ni81	1.85826
C11-C14-C15	120.81278	Cu1-O79	2.52049	Co81-O78	2.33129	Ni81-O75	2.80656
C15-C14-O17	116.76440	Cu1-O76	2.96071	Co81-O75	2.43113	Ni81-O78	2.96267
C11-C14-O17	122.42231	O79-H81	0.97779	O78-H80	0.97781	O75-H76	0.97558
C14-O17H18	107.09255	O79-H80	0.98963	O78-H79	0.98722	O75-H77	0.99241
		O76-H78	0.99090	O75-H77	0.98946	O78-H80	0.99408
		O76-H77	0.97610	O75-H76	0.97683	O78-H79	0.97662

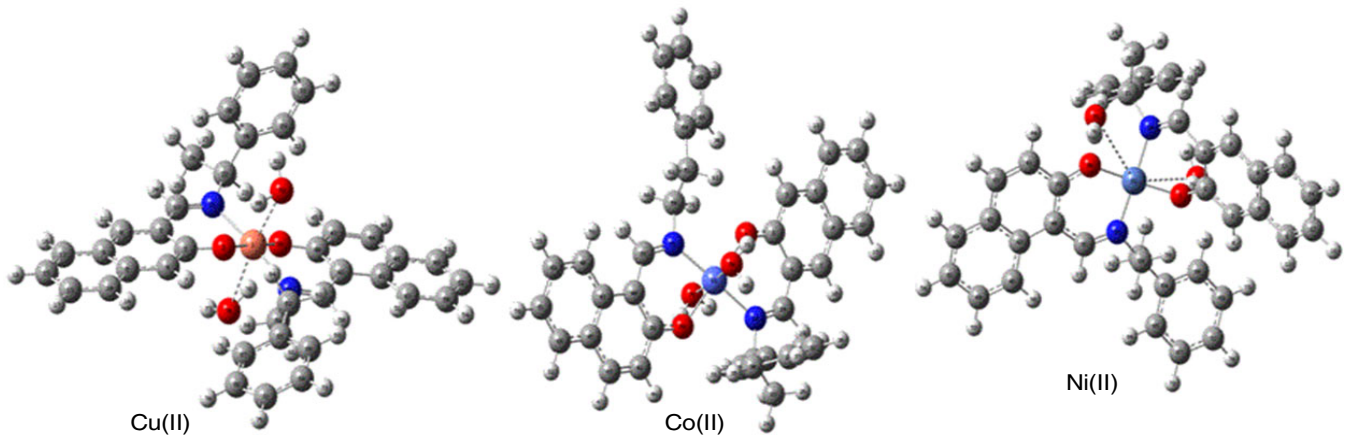

Fig. 3. Optimized structures along with atomic numbering of Cu(II), Co(II) and Ni(II) complexes

system, but it can also be used to calculate the most reactive site in the π-electron system. They are made up of the lowest empty molecular orbitals, known as LUMOs and the highest occupied molecular orbitals, known as HOMOs [27]. The distinction between HOMO and LUMO is that the former is an electron bond giver, while the latter is an electron acceptor. The kinetic stability and electrical characteristics of a molecule are influenced by its HOMO-LUMO molecular orbitals [28]. A lower energy gap correlates with better molecular stability, which is typically linked to low kinetic stability and high chemical resistance. The global electrophilicity power (ω), chemical potential (μ), electron affinity (A), ionization energy (I), global hardness (η) and HOMO and LUMO orbital energies can all be computed using these values [29].

$$A = -E_{LUMO}$$

$$\mu = \frac{E_{HOMO} + E_{LUMO}}{2}$$

$$I = -E_{HOMO}$$

$$\omega = \frac{\mu^2}{2\eta}$$

$$\eta = \frac{(-E_{HOMO\ +\ LUMO})}{2}$$

To determine the orbital energies of the HOMO-LUMO, the 6-311++G(d,p) basis set was utilized for the ligand and the SDD basis set for its metal(II) complexes. The results are summarized in Table-5, accompanied by the visual representations (Figs. 4 and 5). When molecules were examined, the FMO energy gap was found to be in the following order: L > Ni(II) > Co(II) > Cu(II). Thus, the metal complexes exhibit a smaller FMO gap compared to ligands suggests a higher degree of polarizability. Furthermore, the chemical potential of the molecules is more negative, suggesting that the compounds exhibit stability.

MEP analysis: The use of MEP allows for the prediction of the reactive sites for the target molecule being studied. Red indicates the negative electrostatic potential in the MEP diagram, whereas blue indicates the positive electrostatic zones. Green is used to symbolize the neutral electrostatic zone, while yellow is used to symbolize the slightly electron-rich region. The MEP diagram for the molecule being studied, shown in Figs. 6 and 7, illustrates that the electron-rich (red) area extends across the oxygen and nitrogen atoms of the ligand and metal complexes, while the electron-deficient (blue) region is found over

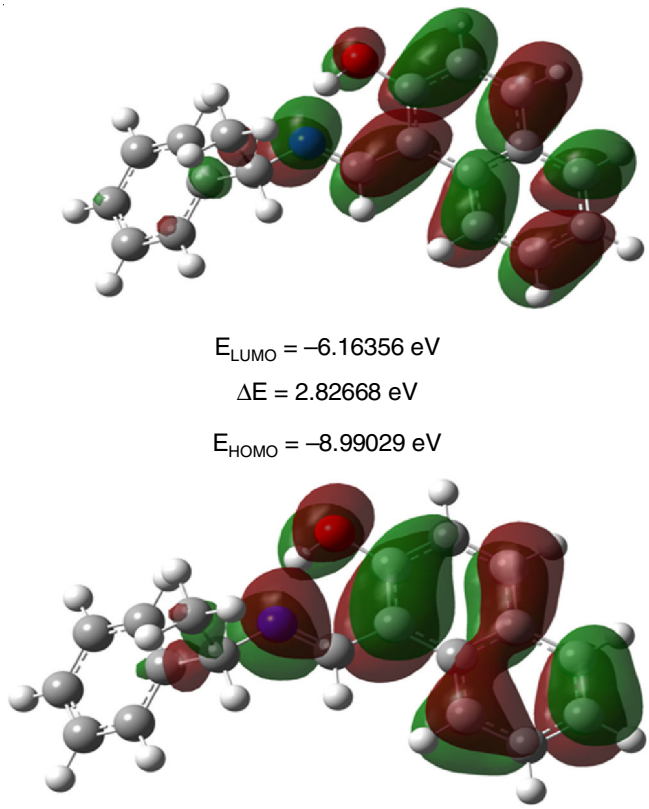

Fig. 4. Frontier molecular orbital of ligand

the hydrogen atom of the ligand and metal moiety. This indicates the possibility of a charge transfer interaction within the molecule to enable its use in the optical devices. The red colour that permeates the oxygen atom within the molecules serves as evidence for the existence of the C-H-O interaction. As a result, it was established that the molecule exhibited an effective charge transfer interaction, making the material suitable for the NLO devices.

Biological evaluation

Antibacterial activity: The antibacterial activity of Schiff base ligand and its Cu(II), Co(II) and Ni(II) complexes against Gram-positive bacteria *Bacillus subtilis* and *Staphylococcus aureus* as well as Gram-negative bacteria *Escherichia coli* and *Pseudomonas putida*, using a disc diffusion method [30,31]. In this study, the results were expressed through minimum inhibitory concentrations (MICs) using ampicillin as a reference compound. The antibacterial activity results for Co(II) and Ni(II) complexes showed good activity against *B. subtilis*

TABLE-5
LIGAND PARAMETERS FMO's AND ITS METAL COMPLEXES

Frontier molecular orbital parameter	Ligand (eV)	Cu(II) (eV)	Co(II) (eV)	Ni(II) (eV)
HOMO energy	-8.99024	-5.80138	-7.69962	-7.72493
LUMO energy	-6.16356	-5.64805	-7.31731	-6.21472
Frontier molecular orbital energy gap	2.82668	0.15332	0.38230	1.51020
Ionization energy (I)	8.99024	5.80138	7.69962	7.72493
Electron affinity (A)	6.16356	5.64805	7.31731	6.21472
Global hardness (η)	1.41334	0.07669	0.19115	0.75510
Chemical potential (μ)	-7.57690	-5.72471	7.50846	-6.96982
Global electrophilicity power (ω)	20.30983	213.7509	147.46806	32.16687

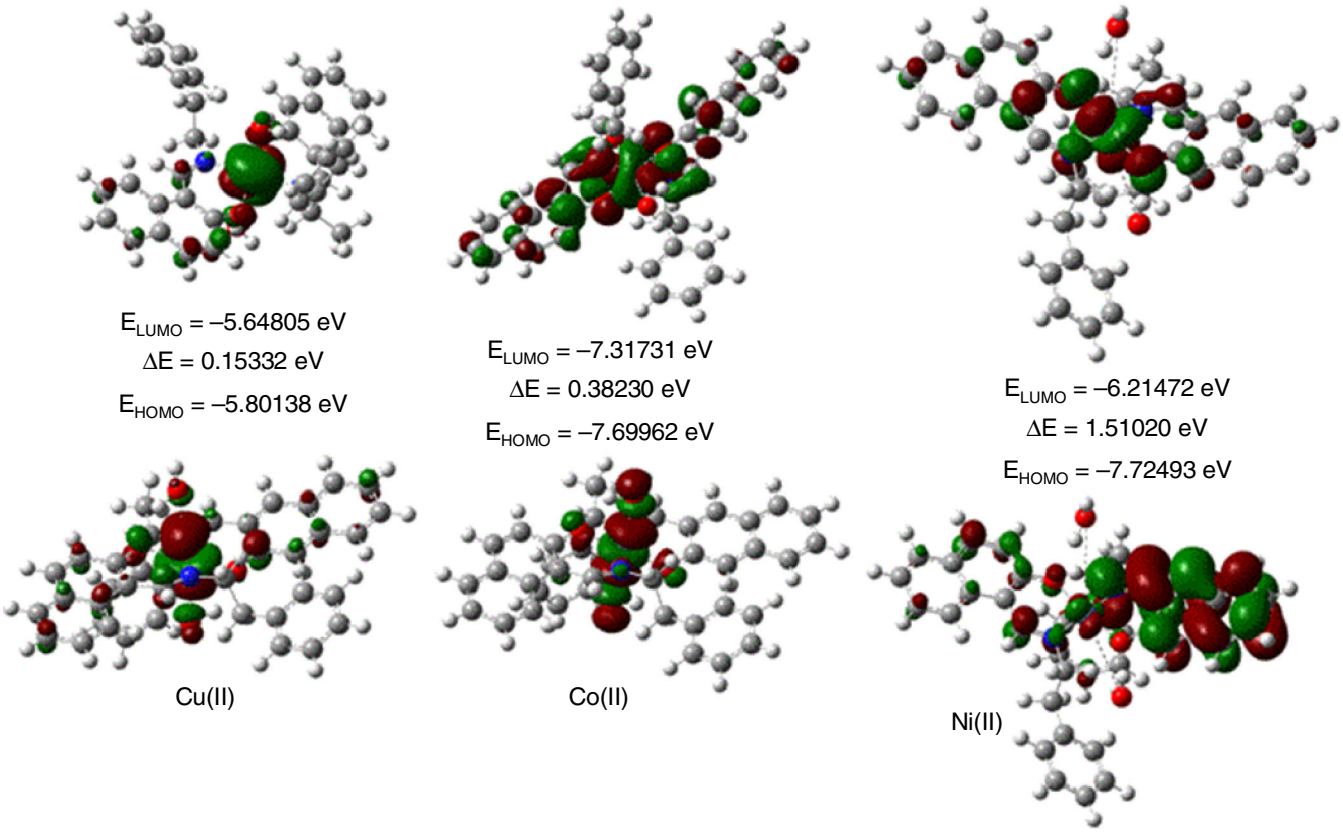

Fig. 5. Frontier molecular orbitals of Cu(II), Co(II) and Ni(II) complexes

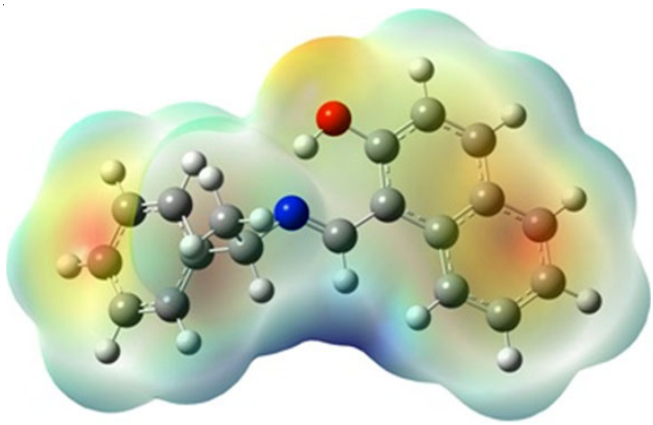

Fig. 6. Electrostatic potential surface ligand plotted with total electron density

and moderate activity against *P. putida* (Table-6). There was minimal interaction between the Cu(II) complex and the ligand against each strain. The DFT calculations validated the antimicrobial results in a significant way. In addition, the Schiff base and complexes were found to inhibit varying degrees of bacterial growth.

TABLE-6
ANTIBACTERIAL ACTIVITY OF COMPOUNDS REPRESENTED IN MIC (μg/mL)

Compound	*B. subtilis*	*S. aureus*	*P. putida*	*E. coli*
Cu(II)	>100	>100	32.74	19.92
Ni(II)	12.5	>100	8.32	>100
Co(II)	10.44	24.83	6.72	18.35
Ligand	35.49	>100	>100	46.11
Control	7.21	9.16	4.73	6.42

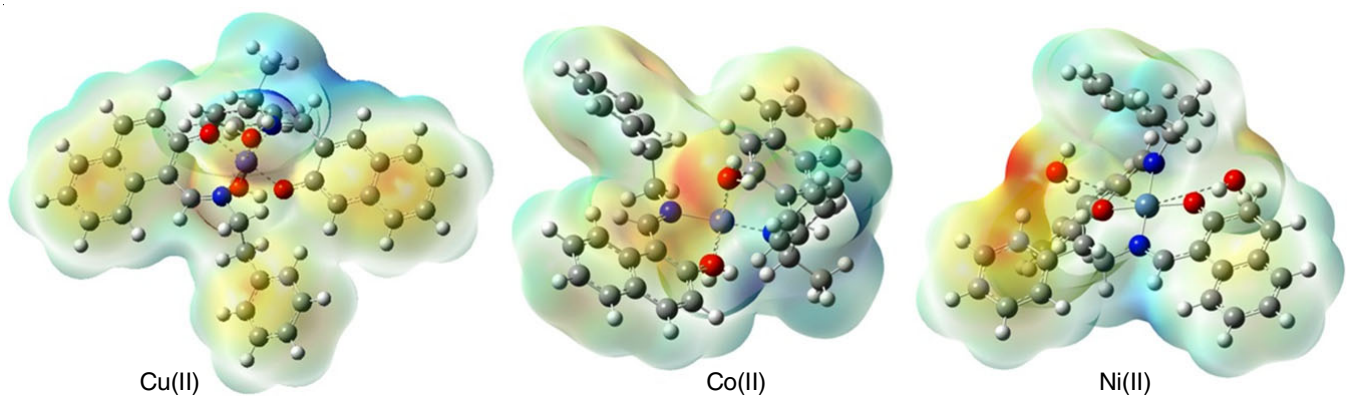

Fig. 7. Electrostatic potential surface of Cu(II), Co(II) and Ni(II) complexes plotted with total electron density

TABLE-7
ANTICANCER ACTIVITY OF LIGAND AND ITS METAL COMPLEXES [*in vitro* (IC_{50}, μM)]

Compound	MCF-7	A549	HepG-2	HeLa	HEK293
Cu(II)	13.50 ± 0.12	11.83 ± 0.22	14.84 ± 1.12	10.10 ± 0.13	87.43 ± 0.21
Co(II)	21.98 ± 1.34	39.71 ± 0.13	15.22 ± 1.24	25.71 ± 0.31	Not determine
Ni(II)	18.99 ± 0.14	16.26 ± 1.11	31.28 ± 0.21	11.93 ± 0.12	Not determine
Ligand	49.73 ± 0.15	53.44 ± 0.13	33.26 ± 0.21	18.44 ± 0.24	Not determine
Cisplatin	8.12 ± 0.12	5.13 ± 0.14	3.11 ± 0.24	6.18 ± 0.12	Not determine

***In vitro* antiproliferative evaluation:** Several human cancer cell lines, such as MCF-7 (breast), A549 (lung), HepG-2 (liver), HeLa (cervical) and HEK293 (embryonic kidney), were tested for anticancer activity *in vitro* using the MTT assay method. The Cu(II) complex generally demonstrated good activity against both HeLa and MCF-7 cells with IC_{50} values between 10.10 and 0.13 μM (Table-7). Based on the findings on anticancer activity, a weak effect was observed against the cell lines, when the Schiff base ligand and its metal complexes were used. Stable compounds are not hazardous, as we showed when assessing the Cu(II) complex against HEK293 cell lines; none of the synthesized compounds impacted the viability of the normal cell lines. The IC_{50} values that were observed were 87.43 ± 0.21 μM.

Conclusion

The Schiff derived from 2-hydroxy-1-naphthaldehyde and N-phenyl ethylamine and its metal(II) complexes were synthesized and characterized analytically and spectroscopically. The theoretical calculations were used to estimate the characteristics of the new Schiff base ligand and its metal(II) complexes. The low LUMO energy supports cell inhibition while low energy band gaps indicate the promising antibacterial activity since the electrical transport capabilities require less energy. Moreover, the antibacterial screening revealed that the Co(II) complex exhibited robust activity against *B. subtilis* and *P. putida* stains, with MIC values of 10.44 and 6.72 μg/mL, respectively. The IC_{50} values of 10.10 ± 0.13 μM and 13.50 ± 0.12 μM against HeLa and MCF-7, Cu(II) complex showed good anticancer activity.

ACKNOWLEDGEMENTS

One of the authors, Jagadish Tota, thanks the CVR College of Engineering and UGC, New Delhi, India, for the financial support.

CONFLICT OF INTEREST

The authors declare that there is no conflict of interests regarding the publication of this article.

REFERENCES

1. Z. Çetin and B. Dede, *J. Mol. Liq.*, **380**, 121636 (2023); https://doi.org/10.1016/j.molliq.2023.121636
2. K., Ramaiah, P.R. Koya, G. Naaresh Reddy and P. Jyothi, *J. Mol. Struct.*, **1263**, 133070 (2022).
3. J. Li, L. Wang, H. Bai, B. Yang and H. Yang, *Med. Chem. Res.*, **20**, 88 (2011); https://doi.org/10.1007/s00044-009-9289-2
4. R. Konakanchi, R. Mallela, R. Guda and L.R. Kotha, *Res. Chem. Intermed.*, **44**, 27 (2018); https://doi.org/10.1007/s11164-017-3089-y
5. R. Konakanchi, G.S. Pamidimalla, J. Prashanth, T. Naveen and L.R. Kotha, *Biometals*, **34**, 529 (2021); https://doi.org/10.1007/s10534-021-00293-1
6. R. Mallela, R. Konakanchi, R. Guda, N. Munirathinam, D. Gandamalla, N.R. Yellu and L.R. Kotha, *Inorg. Chim. Acta*, **469**, 66 (2018); https://doi.org/10.1016/j.ica.2017.08.042
7. R. Gandhaveeti, R. Konakanchi, P. Jyothi, N.S.P. Bhuvanesh and S. Anandaram, *Appl. Organomet. Chem.*, **33**, e4899 (2019); https://doi.org/10.1002/aoc.4899
8. R. Konakanchi, J. Haribabu, J. Prashanth, V.B. Nishtala, R. Mallela, S. Manchala, D. Gandamalla, R. Karvembu, B.V. Reddy, N.R. Yellu and L.R. Kotha, *Appl. Organomet. Chem.*, **32**, e4415 (2018); https://doi.org/10.1002/aoc.4415
9. R. Konakanchi, S. Kankala and L.R. Kotha, *Synth. Commun.*, **48**, 1777 (2018); https://doi.org/10.1080/00397911.2018.1463545
10. R. Konakanchi, V.B. Nishtala, S. Kankala and L.R. Kotha, *Synth. Commun.*, **48**, 2642 (2018); https://doi.org/10.1080/00397911.2018.1506034
11. R. Konakanchi, R. Gondru, V.B. Nishtala and L.R. Kotha, *Synth. Commun.*, **48**, 1994 (2018); https://doi.org/10.1080/00397911.2018.1479758
12. Y. Monika, Y. Deepak, S. Dharam Pal and K. Jitander Kumar, *Inorg. Chim. Acta*, **546**, 121300 (2023); https://doi.org/10.1016/j.ica.2022.121300
13. C. Boulechfar, H. Ferkous, A. Delimi, A. Djedouani, A. Kahlouche, A. Boublia, A.S. Darwish, T. Lemaoui, R. Verma and Y. Benguerba, *Inorg. Chem. Commun.*, **150**, 110451 (2023); https://doi.org/10.1016/j.inoche.2023.110451
14. I. Kostova and L. Saso, *Curr. Med. Chem.*, **20**, 4609 (2013); https://doi.org/10.2174/09298673113209990149
15. A.M. Deghady, R.K. Hussein, A.G. Alhamzani and A. Mera, *Molecules*, **26**, 3631 (2021); https://doi.org/10.3390/molecules26123631
16. S. Murugavel, N. Manikandan, D. Lakshmanan, K. Naveen and P.T. Perumal, *J. Chil. Chem. Soc.*, **60**, 3015 (2015); https://doi.org/10.4067/S0717-97072015000300008
17. K.N. Aneesrahman, K. Ramaiah, G. Rohini, G.P. Stefy, N.S.P. Bhuvanesh and A. Sreekanth, *Inorg. Chim. Acta*, **492**, 131 (2019); https://doi.org/10.1016/j.ica.2019.04.019
18. E. Canpolat, *Polish J. Chem.*, **79**, 619 (2005).
19. P. Zhou, Z.L. You, J. Wang and J. Yang, *Synth. React. Inorg. Met.-Org. Nano-Met. Chem.*, **37**, 219 (2007); https://doi.org/10.1080/15533170701301744
20. M.V. Veidis, G.H. Schreiber, T.E. Gough and G.J. Palenik, *J. Am. Chem. Soc.*, **91**, 1859 (1969); https://doi.org/10.1021/ja01035a051
21. D. Shukla, L.K. Gupta and S. Chandra, *Spectrochim. Acta A Mol. Biomol. Spectrosc.*, **71**, 746 (2008); https://doi.org/10.1016/j.saa.2007.12.052
22. S. Nigam, M.M. Patel and A. Ray, *J. Phys. Chem. Solids*, **61**, 1389 (2000); https://doi.org/10.1016/S0022-3697(00)00025-1
23. C. Lee, W. Yang and R.G. Parr, *Phys. Rev. B Condens. Matter*, **37**, 785 (1988); https://doi.org/10.1103/PhysRevB.37.785
24. C.J. Cramer and D.G. Truhlar, *Phys. Chem. Chem. Phys.*, **11**, 10757 (2009); https://doi.org/10.1039/b907148b
25. N. Kavitha, M. Alivelu and R. Konakanchi, *Polycycl. Aromat. Compd.*, **42**, 5534 (2022); https://doi.org/10.1080/10406638.2021.1939071

26. M.J. Frisch, G.W. Trucks, H.B. Schlegel, G.E. Scuseria, M.A. Robb, J.R. Cheeseman, G. Scalmani, V. Barone, B. Mennucci, G.A. Petersson, H. Nakatsuji, M. Caricato, X. Li, H.P. Hratchian, A.F. Izmaylov, J. Bloino, G. Zheng, J.L. Sonnenberg, M. Hada, M. Ehara, K. Toyota, R. Fukuda, J. Hasegawa, M. Ishida, T. Nakajima, Y. Honda, O. Kitao, H. Nakai, T. Vreven, J. A. Montgomery, Jr., J.E. Peralta, F. Ogliaro, M. Bearpark, J.J. Heyd, E. Brothers, K.N. Kudin, V.N. Staroverov, R. Kobayashi, J. Normand, K. Raghavachari, A. Rendell, J.C. Burant, S.S. Iyengar, J. Tomasi, M. Cossi, N. Rega, J.M. Millam, M. Klene, J.E. Knox, J.B. Cross, V. Bakken, C. Adamo, J. Jaramillo, O. Yazyev, R. Gomperts, R.E. Stratmann, A.J. Austin, R. Cammi, C. Pomelli, J.W. Ochterski, R.L. Martin, K. Morokuma, V.G. Zakrzewski, G.A. Voth, P. Salvador, J.J. Dannenberg, S. Dapprich, A.D. Daniels, Ö. Farkas, J.B. Foresman, J.V. Ortiz, J. Cioslowski and D.J. Fox, Gaussian, Inc., Wallingford CT (2009).
27. R. Arulraj, *J. Mol. Struct.*, **1248**, 131483 (2022); https://doi.org/10.1016/j.molstruc.2021.131483
28. K. Funatsu, T. Miyao and M. Arakawa, *Curr. Computeraided Drug Des.*, **7**, 1 (2011); https://doi.org/10.2174/157340911793743556
29. K. Eswar Srikanth, K. Ramaiah, D. Jagadeeswara Rao, K. Prabhakara Rao, J. Laxman Naik, A. Veeraiah and J. Prashanth, *Indian J. Phys.*, **94**, 1153 (2020); https://doi.org/10.1007/s12648-019-01562-z
30. M. Musthafa, R. Konakanchi, R. Ganguly and A. Sreekanth, *Phosphorus Sulfur Silicon Relat. Elem.*, **195**, 331 (2020); https://doi.org/10.1080/10426507.2019.1699924
31. M. Musthafa, R. Konakanchi, R. Ganguly, P. Pandikumar and A. Sreekanth, *Res. Chem. Intermed.*, **46**, 3853 (2020); https://doi.org/10.1007/s11164-020-04177-w